Proceedings of the Fourth International Symposium
on
ADVANCED NUCLEAR ENERGY RESEARCH
ROLES AND DIRECTION OF MATERIAL SCIENCE IN NUCLEAR TECHNOLOGY

RADIATION DETECTION WITH Nb/Al-AlOx/Al/Nb SUPERCONDUCTING TUNNEL JUNCTIONS

Atsuki Matsumura, Toru Takahashi* and Masahiko Kurakado*
Electronics Research Labs. and Advanced Material & Technology Research Labs*,
Nippon Steel Corp.,
1618 Ida, Nakahara-ku, Kawasaki 211, Japan
Phone 044-777-4111, Fax 044-777-2090

Abstract: Superconductor radiation detectors have the possibility of 20-30 times better energy resolution than that of a high resolution Si detector. We fabricated Nb/Al-AlOx/Al/Nb superconducting tunnel junctions with low leakage current. X rays were detected with large area junctions of 178×178 μm^2. High energy resolution of 160 eV for 5.9 keV was obtained. We also fabricated series connected junctions which covers a rather large area of 4×4 mm^2. α particles injected into the rear substrate were detected using nonthermal phonons induced by the radiations in the substrate.
Keywords: radiation detector, superconductor, superconducting tunnel junction, x ray, α particle, niobium, energy resolution, series-connected STJ detector, nonthermal phonons, ballistic phonons

1. INTRODUCTION

The energy resolution of a radiation detector is fundamentally limited by the statistical fluctuation of the number of charges ionized or excited by a radiation in the detector. Si detectors usually have high resolution with FWHM (full width at half maximum) = 140 eV for 5.9-keV x rays as typical one. In order to obtain much higher energy resolution, one should make use of a material whose ε value, i.e. the mean energy required to excite one electron, is much smaller than that of Si detectors (ε ≃ 3.6 eV). It is, however, empirically well known that the ε value of a semiconductor is (14 / 5) Eg + (0.5 ~ 1.0) eV, where Eg is the gap energy of the semiconductor.

The ε values of low-Tc superconductors have been estimated to be of the order of 1 meV.[1,2] Therefore, with superconductors, we can expect much higher resolution than Si. Furthermore, because the phonons with energy larger than Eg can excite electrons efficiently,[2] superconductor detectors have unique possibilities (a) 20-30 times better energy resolution than that of a high resolution Si detector, and (b) signal appearance not only caused by ionizing interactions but also by nonionizing interactions.

Superconducting tunnel junctions are used to collect electrons excited by radiations in the superconductor. Detectors using Sn junctions have been investigated and detection of α-particles [3], x rays [4, 5] were reported. Sn junctions have low leakage current and recently x rays were detected by Sn junctions with about three times higher energy-resolution than that of semiconductor Si detectors [6]. Though Sn junctions have revealed good characteristics, it is well known that they are easily destroyed by thermal cycles. Since Nb junctions are more resistant to thermal cycles than Sn junctions, radiation detectors using Nb junctions have been investigated recently [7-13]. However, the leakage current of Nb junctions was not sufficiently low enough. Large leakage current brings about a large noise. Thus, only small junctions, smaller than 100 × 100 μm^2, could be used for detection of x rays.

Because of the smallness of the junctions, a part of excited electrons diffuses from the junction to its leads [3]. The amount of the diffused electrons depends on the incident position of radiations. The diffusion of excited electrons from junction area to its leads deteriorates the energy resolution. We fabricated Nb/Al-AlOx/Al/Nb junctions with considerably lower leakage current than those in previous studies and detected x rays using larger area junctions than previous ones.

We also fabricated series connected junctions, which covers rather large area. α particles injected into the rear substrate were detected by using the nonthermal phonons induced by the radiations.

2. X-RAYS DETECTION WITH SINGLE JUNCTIONS [12]

2-1 Samples prepared

Structure of the samples is shown in Fig. 1. Nb junctions were prepared on a sapphire substrate by DC magnetron sputtering. Nb/Al-AlOx/Al/Nb layers were deposited successively. Thicknesses of the junction layers are 2000 Å for the lower Nb

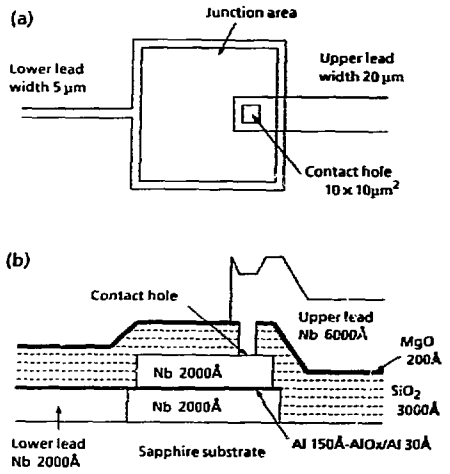

Fig. 1 Sample structures : (a) a plane figure; (b) the cross-sectional view.

layer, 150 Å for the lower Al layer, 30 Å for the upper Al layer and 2000 Å for the upper Nb layer. After the deposition of the lower Al layer, oxygen gas was introduced into the vacuum chamber and Al was thermally oxidized at room temperature. We used a photo-lithography technique (SNIP method [14]) for device fabrication. An upper lead of Nb contacts to the junction through a 10 × 10 μm² contact hole. The width of lower lead is 5 μm and that of upper lead is 20 μm.

X rays were detected with two junctions : junction A, 36.8 × 36.8 μm² and junction B, 178 × 178 μm². They were fabricated on the same substrate. The x-ray source was ^{55}Fe, which emits Mn K x-rays (5.9 keV ; 88%, 6.5 keV : 12%). The operating temperature of junctions was about 0.4 K. The leakage current at the bias voltage of 0.5 mV was 3 nA for junction A and 20 nA for junction B at 0.4 K. The dynamic resistances (dV/dI) at the bias points of junction A and B were 170 kΩ and 20 kΩ, respectively. Normal resistances of the junctions were 3.5 Ω for junction A and 0.14 Ω for junction B. The signals from a junction were fed to a charge-sensitive preamplifier. The outputs of the preamplifier were transferred to a multichannel analyzer through a main amplifier.

2-2 Results of x-ray detection

An x-ray spectrum obtained with junction A is shown in Fig.2(a). The effective ε value (εeff) defined by εeff = $E/(Q/e)$ was about 24 meV for 5.9-keV x rays, assuming channel 156 corresponds to 5.9 keV in Fig. 2(a). Here E is the energy of the radiation, Q is the signal charge and e is the charge of electron. This εeff value corresponds to about 150 times larger signal charge than that from a semiconductor Si detector (ε = 3.6 eV). However, the energy resolution is not good probably because of the diffusion of excited electrons. The broadness of spectrum due to noise was measured by supplying pulser signals to the test input of the preamplifier. The full width at half maximum (FWHM) of pulser peak is about 41 eV.

Fig. 2(b) shows an x-ray spectrum obtained with junction B. The voltage gain of the main amplifier is different from the case of Fig. 2(a). It is well known

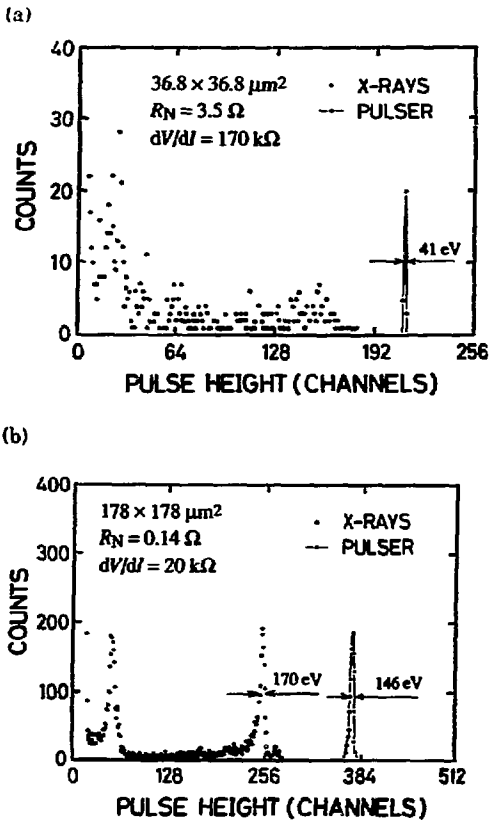

Fig. 2 Pulse height spectra for x rays from ^{55}Fe (5.9 keV : 88 %, 6.5 keV : 12 %) and pulser signals obtained with (a) junction A, 36.8×36.8 μm²; (b) junction B, 178×178 μm². The counts for pulser signals are out of scale.

that the amount of the signal charge arising from one of the superconductor layers depends on the thickness and qualities of the layer [4,5,9]. In the vicinity of channel 256 in Fig. 2(b), two sharp peaks are observed. Another sharp peak is also observed in a low energy region in the spectrum. At present, we do not know which layer produced the higher side peaks. Hereafter we only discuss the higher side peaks.

Peaks corresponding to 5.9 keV and 6.5 keV are apparently separated from each other. The Eeff is about 26 meV at 5.9 keV. The signal charge for 5.9-keV x rays is about 135 times larger than that from a Si detector. The FWHM of the 5.9-keV x-ray peak is about 170 eV. The broadness of the pulser peak is about 146 eV. This value is larger than that of junction A, because the leakage current and the electric capacitance of junction B were larger than those of junction A. Nevertheless, the energy resolution of junction B is much better than that of junction A. Since the size of junction B is much larger than that of junction A, the effect of energy diffusion is effectively suppressed in the case of junction B.

We fabricated many types of junctions on one substrate, including two 178 × 178 μm² junctions. X ray spectrum obtained with the other junction of 178 × 178 μm² on the same substrate as junction B is shown in Fig. 3. The FWHM of the 5.9-keV x-ray peak is about 160 eV, which is the best energy resolution obtained with Nb junctions so far.

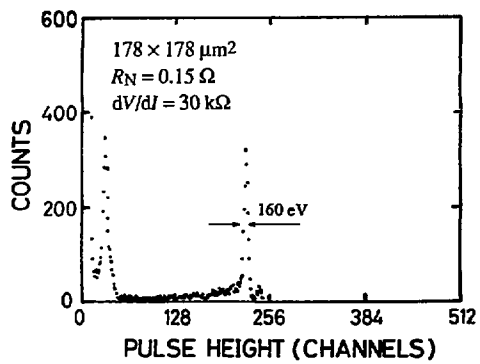

Fig. 3 Pulse height spectra for x rays from ^{55}Fe (5.9 keV : 88 %, 6.5 keV : 12 %) obtained with the other junction of 178×178 μm² on the same substrate as junction B.

3. α-PARTICLE DETECTION WITH SERIES-CONNECTED JUNCTIONS [13]

3-1 Series connection of junctions

Since the sensitive area of superconducting tunnel junctions (STJs) used in the previcus works was very small, i.e., on the order of or less than 100×100 μm², their detection efficiencies were too low for practicai use. For further development, it is clearly necessary to make STJs with a much larger sensitive region. However, the low resistivity and the large capacitance, inherent in STJ (typically 10-5 Ω·cm² and 10 μF/cm²), make it very difficult to fabricate large superconductor detectors.

One of the possible methods to increase the sensitive area of superconductor detectors is to use an assembly of STJs connected in series on one substrate. An apparent benefit of the series connection of STJ elements is the great enhancement of the electric resistance of detectors. Furthermore, the capacitance of the detector can be relatively diminished by the series connection. In this section, we review the series connected STJ detector, which is designed as a sensor of nonthermal phonons excited by collision of high-energy radiations with the rear substrate.

3-2 Effective capacitance of a series-connected STJ detector

From a simple model of uniform STJs connected in series, the effective capacitance defined by (signal charge / signal voltage) is given by $C+n\cdot C'$. C is the capacitance of one STJ element, n is the number of STJs and C' is the sum of the capacitances parallel to the detector, i.e., capacitances of a preamplifier and signal cables. Consequently,

$$Ceff = S\cdot C_0 / n + n\cdot C',$$

where S is the total area of the STJs and C_0 is the junction capacitance per unit area. Therefore, $Ceff$ takes its minimum value of

$$2(S\cdot C_0\cdot C')^{1/2} \quad \text{when} \quad n=(S\cdot C_0 / C')^{1/2}.$$

The minimum value is usually much smaller than $S\cdot C_0+C'$, especially for large S.

3-3 Detection of nonthermal phonons

Electrons in the superconductive state of STJ are efficiently excited by nonthermal phonons with energies

$$\Omega \geqq 2\Delta$$

where Ω is the energy of the phonon and 2Δ is the gap energy, which is defined as a minimum energy necessary to excite two electrons by destroying a Cooper pair. As shown by Kurakado[2], the number of electrons excited by a phonon is approximately proportional to the energy Ω and $\varepsilon \simeq 1.7\Delta$. This high sensitivity to nonthermal phonons can be applied to measure full energies of high-energy radiations such as α particles. In our work, the series-connected STJ

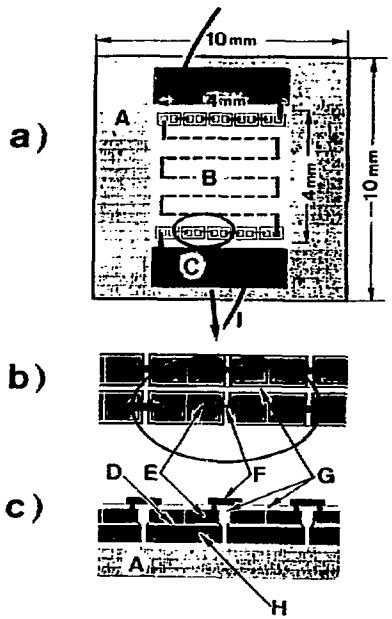

Fig. 4 Schematic drawings of the series-connected STJ detector: (a) a plane figure; (b) the enlargement of a part of the STJ assembly; (c) the cross-sectional view of the STJ assembly. Notations in the figures: A, sapphire substrate (10×10 mm²); B, assembly of STJ elements connected in series (4×4 mm²); C, electrode; D, aluminum oxide barrier; E, top layer (Nb); F, contact leads (Nb); G, insulator (SiO); H, bottom layer (Nb); I, electrical lead.

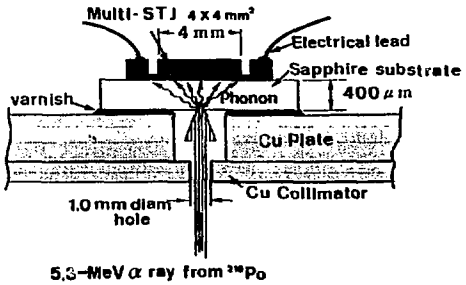

Fig. 5 Experimental setup to test the series-connected STJ detector. The rear sapphire substrate is irradiated by collimated α particles. An assembly of STJs at the front side is used as a sensor for nonthermal phonons generated by the collision of α particles. The area size of the STJ assembly is 4×4 mm².

detector has been used as a sensor to detect nonthermal phonons created by irradiation of its rear substrate with nuclear radiations. In addition to ionizing events, such phonons are created also through nonionizing events such as elastic scattering processes[2], which cannot be sensed by ordinary radiation detectors. Note that the series-connected STJ detector is sensitive to the nonionizing events as well as the ionizing events.

The series-connected STJ detector is similar to the silicon crystal acoustic detector (SiCAD),[15,16] which is also the phonon sensor composed by many STJs. Each STJ in SiCAD is operated independently, while all STJs in our detector work as one phonon sensor through the connection in series.

3-4 Experimental setup

Layout of the series-connected STJ detector is given by Fig. 4. An array of micro STJ elements in the detector is schematically shown in Fig. 4(a); the sensitive area covered with the STJ elements is 4×4 mm² while the area of one STJ element is 20×20 or 100×100 μm². All STJ elements in the detector are connected in series, as shown in Fig. 4(b). Each STJ element consists of Nb/Al-AlOx/Nb layers, which are shown in Fig. 4(c). The bottom Nb layers of all samples were epitaxially formed on a sapphire substrate by using molecular beam epitaxy (MBE) system[9]. This is preferable for sensing phonons coming from the substrate.

The experimental setup to detect α particles with the series-connected STJ detector is shown by Fig. 5. The rear side of the substrate is irradiated by 5.3 MeV ^{210}Po α particles which are collimated by a 1-mm-diam hole of a 1-mm-thick copper plate. The whole energies of α particles are absorbed at the surface of the sapphire substrate and are immediately transferred to energies of nonthermal phonons. Those phonons were detected by the STJ elements on the front side. Signals from the detector cooled at 0.4 K in a cryostat are fed to a charge-sensitive preamplifier mounted outside the cryostat.

3-5 Samples prepared

Three samples (A, B and C) of the series-connected STJ detector were prepared. Some properties of each sample are listed in Table 1, i.e., size of an STJ, number of STJs n, total area of STJs, dynamic resistance of sample R_d and effective capacitance of sample C_{eff}. The dynamic resistance R_d is defined by the differential dV/dI at $V=0$, which was determined from the I-V curve measured at 0.4 K. The normal resistivity of junction is ~5×10^{-6} Ωcm² for all samples. The rather large value 250 pF for C' comes from the preamplifier used, which is commercially available and is designed for surface-barrier semiconductor detectors with large input capacitance ; the noise level is 2 keV for Si (ε=3.6 eV and C=0 pF) and the input capacitance is ~200 pF.

Table I. Properties of each sample [13].

Sample	Size of an STJ (μm^2)	Number of STJs n	Total area of junctions (mm^2)	R_d (kΩ)	C_{eff} (μF)
A	20x20	8000	3.2	100	2.0
B	100x100	960	9.6	2	0.24
C	100x100	960	9.6	100	0.24

3-6 Results of α-particle detection

Some features of signals from each sample are summarized in Table II ; height, risetime, decay time, signal charge (Q) and the effective ε value (εeff). The risetime is rather fast (~1 μs); this indicates that nonthermal ballistic phonons excited by radiations are transmitted sufficiently fast in the single crystal of sapphire substrate.

The pulse height spectra of 5.3 MeV α particles obtained with the samples are shown in Fig. 6; the experimental arrangement for the samples is given by Fig. 5. The broadness due to electronic noises is indicated by the pulser peak in each spectrum, which was obtained by supplying pulser signals to the test input of the preamplifier.

The number of STJs in sample A, 8000, is so large that C_{eff} (2.0 μF as seen in Table I) becomes large. In spite of the large capacitance of this sample, the large resistance caused by the connection of STJs in series practically made it possible to detect α particles. Output signal height was small as seen in Table II. FWHM of the pulser peak was 1140 keV.

In the case of sample B or C, the number of STJs is improved and C_{eff} is comparably small (0.24 μF as seen in Table I). Therefore the heights of output signal become large as seen in Table II. A main difference between samples B and C is the leakage current, as seen in Table I ; the leakage current of

Table II. Preamplifier outputs of each sample [13].

Sample	Height (mV)	Risetime (μs)	Decay time[a] (μs)	Q (pC)	ε_{eff}[b] (meV)
A	~1	----	---	18	47
B	40	~0.6	19	90	9.4
C	45	~0.6	200	100	8.5

[a] Intrinsic decay time of the preamplifier is 550 μs.

[b] $\varepsilon_{eff}=E/(Q/e)$.

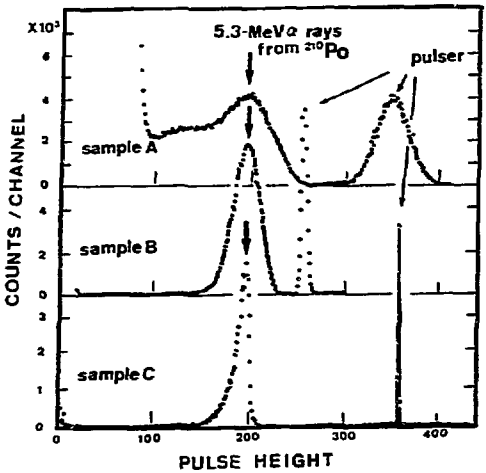

Fig. 6 Pulse-height spectra of electric signals induced by 5.3 MeV α particles on samples A, B, and C, which were obtained with the experimental setup shown by Fig. 5.

sample C is decreased to one fiftieth of that of sample B. This is a reason that the FWHM of pulser peak with sample C is improved from 200 keV with sample B to 34 keV and also why the decay time of output signals is prolonged from 19 to 200 μs, as seen in Table II.

The energy resolution obtained by the best sample C is still not sufficient, suffering from the escape of phonons from the detector and perhaps nonuniformity of junction properties in the detector. A method to attenuate the effect of phonon escape is to make samples with larger sensor regions; the series-connected STJ detector as large as 1×1 cm^2 can be fabricated with our present technique With such large detector, it may be possible to make clear the degree of the similarity of junction properties in the detector prepared by our technique. The effective capacitance C_{eff} can be greatly decreased by employing a preamplifier system with lower input capacitance and samples precisely optimized for the number of STJ elements, which may improve more the signal-to-noise ratio of pulse height spectra. For example, $C_{eff}=0.022$ μF is possible with values of $C'=20$pF, $C_0=6$μF/cm^2 and $S=1cm^2$.

The study of series-connected STJ detectors has been performed in cooperation with Dr. Shin Ito, Dr. Rintaro Katano and Dr. Yasuhito Isozumi of Kyoto University.

References

[1] M. Kurakado and H. Mazaki, Nucl. Instr. and Meth. 185, 141 (1981).

[2] M. Kurakado, Nucl. Instr. and Meth. 196, 275 (1982).

[3] M. Kurakado, J.Appl. Phys. 55, 3185 (1984).

[4] H. Kraus, Th. Peterreins, F. Pröbst, F. von Feilitzsch, R. L. Mössbauer, V. Zacek and E. Umlaut, Europhys. Lett. 1, 161 (1986).

[5] D. Twerenbold, Europhys. Lett. 1, 209 (1986).

[6] W. Rothmund an A. Zehnder : A. Barone ed., "Superconductive Particle Detectors" World Scientific, Singapore, 1988, 52.

[7] M. Kurakado and A. Matsumura, Jpn. J. Appl. Phys. 28, L459 (1989).

[8] M. Kurakado and A. Matsumura, Sensors and Actuators A 21-23, 33 (1990).

[9] M. Kurakado, T. Takahashi and A. Matsumura, Appl, Phys. Lett. 57, 1933 (1990).

[10] P. Gare, R. Engelhardt, A. Peacock, D. Twerenbold, J. Lumley and R. E. Somekh, IEEE Trans. Magn. MAG-25, 1351 (1989).

[11] K. Ishibashi, K. Takeno, Y. Oae, T. Sakae, Y. Matsumoto, A. Katase, S. Takada, H. Akoh and H. Nakagawa, IEEE Trans. Magn. MAG-25, 1354 (1989).

[12] A. Matsumura, T. Takahashi and M. Kurakado, Nucl. Instr. and Meth. A309, 350 (1991).

[13] M. Kurakado, A. Matsumura, T. Takahashi, S. Ito, R. Katano and Y. Isozumi, Rev. Sci. Instrum, 62, 156 (1991).

[14] A. Shoji, S. Kosaka, F. Shinoki, M. Aoyagi and H. Hayakawa, Appl. Phys. Lett. 41, 1097 (1982).

[15] B. Neuhauser, B. Cabrera, C. J. Matoff and B. A. Young, IEEE Trans. Magn. MAG-23, 469 (1987).

[16] Th. Peterreins, F. Pröbst, F. v. Feilitzsch, R. L. Mössbauer and H. Kraus, Phys. Lett. B202, 161 (1988).